

Unsupervised Domain Adaptive Learning via Synthetic Data for Person Re-identification

Qi Wang, *Senior Member, IEEE*, Sikai Bai, Junyu Gao, *Member, IEEE*, and Yuan Yuan, *Senior Member, IEEE*,

Abstract—Person re-identification (re-ID) has gained more and more attention due to its widespread applications in intelligent video surveillance. Unfortunately, the mainstream deep learning methods still need a large quantity of labeled data to train models, and annotating data is an expensive work in real-world scenarios. In addition, due to domain gaps between different datasets, the performance is dramatically decreased when re-ID models pre-trained on label-rich datasets (source domain) are directly applied to other unlabeled datasets (target domain). In this paper, we attempt to remedy these problems from two aspects, namely data and methodology. Firstly, we develop a data collector to automatically generate synthetic re-ID samples in a computer game, and construct a data labeler to simultaneously annotate them, which free humans from heavy data collections and annotations. Based on them, we build two synthetic person re-ID datasets with different scales, namely, “GSPR” and “mini-GSPR” datasets. Secondly, we propose a synthesis-based multi-domain collaborative refinement (SMCR) network, which contains a synthetic pretraining module and two collaborative-refinement modules to implement sufficient learning for the valuable knowledge from multiple domains. Extensive experiments show that our proposed framework obtains significant performance improvements over the state-of-the-art methods on multiple unsupervised domain adaptation tasks of person re-ID.

Index Terms—Person re-identification, domain adaptation, collaborative refinement, synthetic data generation.

I. INTRODUCTION

PERSON re-identification (Re-ID) aims at identifying images of the same pedestrian across non-overlapping camera views in different places, which has attracted a lot of research interests since the urgent demand for public safety and the increasing number of surveillance cameras. Benefiting from the development of deep learning [1], [2] and the availability of labeled re-ID datasets [3]–[5], CNN-based re-ID methods [6]–[9], have made remarkable performance improvements in a supervised manner. However, the aforementioned approaches need a multitude of accurately labeled and diversified data to learn the discriminative features, and the current datasets are not able to perfectly satisfy the demands in dataset scale or data diversity. For example, Market1501 [3] is only collected by six cameras during the summer vacation, and DukeMTMC-reID [4] only contains samples captured by eight cameras in frigid scenes. Meanwhile, all data contained in these datasets are only recorded on the university campus. It causes a tricky problem that the re-ID models trained on these

Q. Wang, S. Bai, J. Gao, Y. Yuan and X. Li are with the School of Artificial Intelligence, OPTics and Electronics (iOPEN), Northwestern Polytechnical University, Xi’an 710072, P.R. China. E-mail: crabwq@gmail.com, whitesk1973@gmail.com, gjy3035@gmail.com, y.yuan1.ieec@gmail.com.

TABLE I
STATISTIC OF REAL-WORLD AND SYNTHETIC PERSON RE-ID DATASETS.
“VIEW” DENOTES WHETHER THE DATASET HAS VIEWPOINT LABELS

Datasets		#box	#identity	#cam	view
real data	Market-1501	32,688	1,501	6	N
	Market-1203	8,569	1,203	2	N
	CUHK03	14,096	1,467	2	N
	DukeMTMC-ReID	36,441	1,812	8	N
	MSMT17	126,441	4,101	15	N
synthetic data	SOMAsset	100,000	50	-	N
	SyRI	1,680,000	100	-	N
	PersonX	273,456	1,26	6	Y
	GPR	443,352	754	12	Y
	mini-GSPR	27,040	520	13	Y
	GSPR	625,416	2,369	26	Y

datasets produce a large performance degradation in unseen extreme cases (e.g., different viewpoints, variant low-image resolutions, illumination changes, *etc*). Moreover, because it may violate people’s privacy, the collection and annotation of re-ID data collection and annotation also become more and more difficult in real world. Regardless of the infringement of people’s privacy, it is impractical to continuously annotate person identities in various new target domains.

In order to address the aforementioned issues, many attempts have been made in terms of data and method. Specifically, from the perspective of data, some approaches have been proposed to make use of commercial software to construct synthetic re-ID datasets [10]–[12]. Leveraging synthetic datasets is a meaningful attempt to remedy the reliance on large-scale real datasets, and the constructed datasets are usually utilized to provide the effective initialization for re-ID models. However, as shown in Table I, existing synthetic data sets suffer from limited data volume or scarce diversity to some extent, and there exist serious differences between synthetic and real datasets due to unrealistic personal characteristics and scenes. It leads to sub-optimal initialization, and there is a poor performance when directly performing the domain adaptive person re-ID tasks from the synthetic datasets to the real-world scenarios.

From the perspective of methodology, unsupervised domain adaptation (UDA) for person re-ID has been proposed, which aims at tackling domain discrepancy between different datasets. There are two main research directions for this problem. The first are domain translation-based methods, which focus on the translation from source domain to target domain by resorting to generating source-to-target samples [5], [13],

[14], where the generated samples inherit ground-truth identity labels from the source domain data and have a similar style with the target domain data.

However, source domain knowledge is simply abandoned after domain translation, and there are no auxiliary pseudo-labels for target domain data in these approaches. The second ones are pseudo label-based methods, which alternately generate pseudo labels by clustering samples from the target domain and train the network with generated pseudo-labeled data [15]–[18]. Although this pipeline has achieved remarkable performance, noisy pseudo-labels and large domain gaps between source and target domains hinder performance further improvements.

In this paper, we attempt to remedy the above problems from two aspects, namely data and methodology. From the data view, we develop a data collector and labeler with the help of a popular electronic game "Grand Theft Auto V" (abbreviation as GTA V), which can be used to generate synthetic pedestrian samples and automatically annotate samples. Based on them, we first build a large-scale synthetic person re-ID dataset, named as "GTA V Synthetic Person Re-ID" (GSPR) dataset. Compared with existing person re-ID datasets, our GSPR has the following advantages: 1) This is a more large-scale person re-ID dataset that consists of 625416 images and a total of 2369 identities across 26 non-overlapping cameras. 2) It is free of collection and annotation, which can liberate people from the labor-intensive collection and annotation of large amounts of data. 3) It is a diversified dataset and considers various extreme cases in real-world scenarios, such as multiple viewpoints, varying image resolutions, illumination changes, unconstrained poses, occlusions, *etc.* Moreover, we construct a mini-scale person re-ID dataset, called "mini GTA V Synthetic Person Re-ID" (mini-GSPR) dataset, which has high resolution and only considers various ideal visual factors. The detailed statistics are illustrated in Table 1.

From the methodological view, we propose a synthesis-based multi-domain collaborative refinement (SMCR) network to improve the performance in domain adaptive person re-ID tasks. There are three strategies in the SMCR network to achieve the goal. Firstly, conventional re-ID methods are pre-trained on ImageNet or synthetic datasets. Due to severe differences between synthetic and real datasets and monotonous pretraining in a single domain, they might be not the optimum option for domain adaptive tasks. To this end, we design a novel pretrained scheme, which exploits the constructed synthetic datasets to pre-train the domain adaptive model by combining source domain data. Considering the serious shift between synthetic and real datasets, we generate synthetic-to-source samples by performing domain translation between synthetic data and source domain. Essentially, our scheme regards the pretrained process as the performance generalization from synthetic-to-source samples to the source domain, and it is able to provide better initialization for domain adaptive models.

Furthermore, we construct two synchronous training and collaborative refinement modules, namely domain translation hybrid refinement (DTHR) module and relation invariant hybrid refinement (RIHR) module. The devised two modules aim

to reduce the negative impacts of the domain gap and preserve original information in the source domain, respectively. DTHR contains a domain translator, a feature encoder, and a pseudo-label generator, which integrates the processes of domain translation and pseudo label prediction, while performing joint training with the generated style-transferrer samples and target domain data. RIHR contains a feature encoder and a pseudo-label generator, which aims to maintain the original inter-instance relations invariant and implement joint learning for the source and target data. Finally, due to the similar architecture and complementary roles between DTHR and RIHR, we introduce a collaborative refinement strategy to further optimize the generated pseudo-labels and the discrimination of target features. Besides, we are sorting out the proposed synthetic datasets and the source code for SMCR, which will be released later.

The major contribution of our work can be summarized as three-fold:

- 1) **Datasets.** Two different scale synthetic person re-ID datasets (i.e., GSPR and mini-GSPR) are constructed with the help of our designed data collector and labeler. There is no labor-intensive cost in the data generation pipeline. Compared with the existing person re-ID datasets, GSPR is a more large-scale and diversified synthetic dataset, and mini-GSPR has higher resolution and more ideal visual conditions. Our datasets effectively relieve the dependence on large-scale real labeled datasets and alleviate the difficulty of domain adaptation.
- 2) **Methodology.** We propose a synthesis-based multi-domain collaborative refinement (SMCR) network to sufficiently exploit the valuable knowledge from multiple domains, which includes a synthetic pretraining module and two collaborative-training modules. The SMCR network not only reduce the adverse impacts of domain discrepancy, but provides a novel learning scheme by utilizing synthetic data for domain adaptive tasks.
- 3) **Experiments.** Extensive experiments are performed on multiple unsupervised domain adaptation tasks of person re-ID, which demonstrate the proposed SMCR obtains consistently optimal performance to the state-of-the-art approaches. We perform ablation studies to verify that all the proposed components contribute to domain adaptive performance.

II. RELATED WORKS

In this section, we first review the previous works about synthetic data, and then briefly describe unsupervised domain adaptation and its applications on person re-ID.

A. Synthetic Data

Manually collecting and labeling an ideal dataset in the real environment is extremely time-consuming and labor-intensive, and it is probably to violate people's privacy. Because unlimited samples can be generated by utilizing sythetic data collector and labeler in theory, many attempts have been made to construct synthetic datasets and alleviate the dependence on

large-scale real labeled datasets. This strategy has been applied in problems like semantic segmentation [19], [20], pose estimation [21], [22], crowd counting [23], [24], *etc.* In the person re-ID, [11] proposed a synthetic instance dataset SOMAset by resorting to photorealistic human body generation software, which contains 50 person models and 11 types of outfits. [25] introduced SyRI dataset using 100 virtual humans illuminated with rich HDR environment maps. In addition, [10] presented a large-scale synthetic dataset named PersonX, which has 1,266 hand-crafted identities and 6 different scenes with multiple viewpoints. Recently, [26] constructed a GPR dataset, which includes 754 identities across 12 non-overlapping cameras. In GPR dataset, the number of cameras and the data volume are still not enough, and the author only designed a coarse data filter based on this dataset to manually select some specific scenes for different datasets. Moreover, the above synthetic datasets are either uneditable or not released to the public.

Comparatively, the proposed synthetic datasets (i.e., GSPR and mini-GSPR) have more diversified scenes, identity categories and data volume. Moreover, various visual factors contained in the constructed datasets can be freely edited/extend, including scenes, weathers, illuminations, data volume, *etc.*, which are not limited to this specific study, and can also be extended to future research in other areas.

B. Unsupervised Domain Adaptation

Unsupervised domain adaptation (UDA) defines a learning problem, where the learned knowledge from the labeled source domain is generalized to the target domain with unknown classes, in order to properly measure the inter-instance affinities of the target domain. Early approaches focused on feature/sample mapping between source and target domains [27], [28]. The respective work, correlation alignment (CORAL) [27], aligned the covariance and mean between source- and target-domain distributions. Furthermore, some methods aim to find domain-invariant feature spaces [29], [30]. [31] and [32] designed the Maximum Mean Discrepancy (MMD) to extract domain-invariant features. [30] and [29] proposed domain confusion loss for this purpose.

Recently, some researchers introduced adversarial learning and pseudo-label generation strategies to reduce the differences between data distributions of source and target domains. Adversarial learning based methods [33], [34] introduced a cycle consistency loss by DiscoGAN [35], DualGAN [36], and CycleGAN [37] to train a domain generator and discriminator to eliminate the discriminative domain information from the learned features. CYCADA [34] transferred the input samples across domains at both pixel- and feature-level. The pseudo-label generation based approaches [38]–[40] focused on modeling relations between unlabeled target domain instances using the predicted pseudo-label. However, the above approaches only focused on conventional domain adaptation for close-set recognition, where the source and target domains share the same label set, and they are not suitable for unsupervised domain adaptation on person re-ID.

C. UDA on person re-ID

Unsupervised domain adaptation (UDA) for person re-ID is an open-set problem, which has disjoint person identity systems between source and target domains. There are extensive studies in unsupervised domain adaptive person re-ID. Domain alignment-based methods tried to minimize the data distribution of the source and the target domain. [41] utilized Maximum Mean Discrepancy (MMD) distance to align the distributions of the source's and the target's mid-level features. [42] applied additional attribute annotations to align feature distributions in common space. Furthermore, domain translation-based methods applied generative adversarial network to generate style-transferred samples with a similar style to the target domain, where the re-ID model is pre-trained in labeled style-transferred samples to perform finetuning in the target domain. PTGAN [5] and SPGAN [43] maintained the ID-related features invariant by utilizing identity-based regularization. SDA [44] used online relationship consistency regularization term to maintain inter-sample relations. Moreover, ATNet [45], CR-GAN [14] and PDA-Net [46] are effective to transfer images with identity labels from source into target domains to learn domain-invariant features. These methods aimed to preserve the original IDs or inter-sample relations during translation, and provide a plausible way to reduce domain gaps between source and target domain by generating style-transferred samples. But the source domain data is simply discarded after translation, and there are no pseudo-labels for target domain data in these strategies. In fact, experimental evidence in [44] and [47] has verified that original inter-sample relations in the source domain and pseudo labels in the target domain are indispensable for cross-domain person re-ID tasks.

The pseudo-label-based approaches [47]–[50] performed feature learning in the unlabeled target domain by utilizing the generated pseudo labels, which have attracted much attention since the very limited cost of manual annotations and state-of-the-art performance. Specifically, the pseudo labels is able to be generated by either clustering features or measuring similarities with exemplar features. PUL [51] designed a cluster and self-pace training framework. SSG [49] assigned multi-scale pseudo labels by utilizing human local features. PAST [16] introduced a progressive training strategy. AD-Cluster [18] incorporated style-translated sample into clustering to improve the discriminativeness of instance features. Moreover, MMT [50] and SPCL [47] introduced mutual learning and self-paced learning respectively to further optimize the pseudo labels. Nevertheless, the above methods cannot sufficiently exploit all valuable knowledge from multiple domains. Most of these methods suffer from the adverse impacts of domain gap and noisy pseudo label.

In addition to considering the discrepancy between different domains, there are some works to camera differences within the single domain. [52] presented a camera-aware similarity consistency loss to learn consistent pairwise similarity distributions for intra-camera matching and cross-camera matching. [4] develop camera-aware domain adaptation framework to reduce the discrepancy between both domains and cameras.

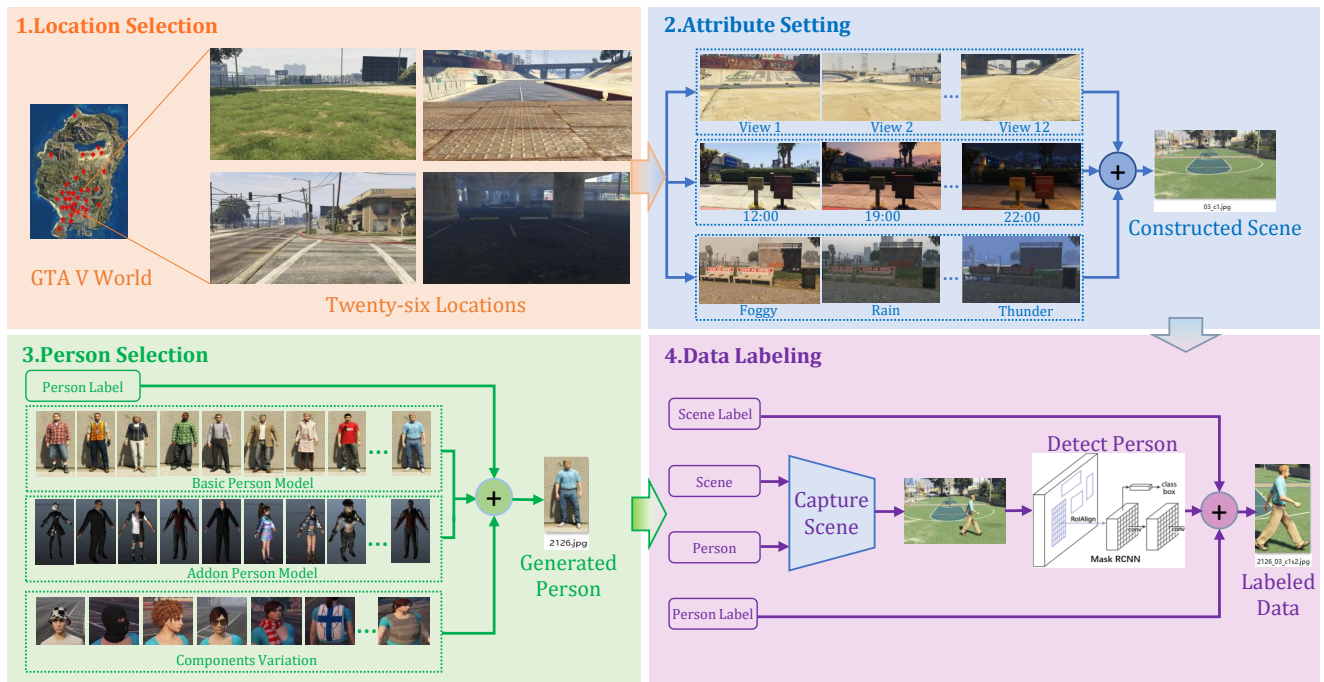


Fig. 1. The pipeline of data generation in GTA 5, including location selection, attribute setting, person selection and data labeling.

[53] introduced camera style adaptation to produce images with different camera styles. [54] trained a camera re-ID model to calculate a camera distance matrix. However, these methods are either only implemented on the target domain, or need to generate massive training data. And there are still few cameras in the current datasets.

III. GTA5 SYNTHETIC PERSON RE-ID

In this section, we first describe the data generation pipeline based on GTA5. As shown in Fig. 1, the pipeline are mainly divided into four parts (*i.e.*, location selection, attribute setting, person selection and data labeling). Then we construct a large-scale synthetic dataset and analyze its detailed properties. Finally, a mini dataset with ideal visual factors is introduced to expect to achieve excellent performance under the condition of delicate design and small data volume.

A. Data Generation

Location Selection. Grand Theft Auto V (GTA5) is a computer game published in 2013. In GTA5, game developers construct a virtual world, which covers an area of 252 square kilometers and contains various visual factors close to real-world conditions. Besides, the game allows players to freely roam to explore abundant gameplay content. In the virtual world of GTA5, we selected 35 typical locations as the background of the synthetic person re-ID data, including mall, street, plaza, mountain, and so on.

Attribute Setting. Following the scene selection, we need to set some essential parameters for each location. Firstly, inspired by [10], since the different views of each person contain different nontrivial details, we set multiple viewpoints in each location, where each viewpoint contains multiple

parameters with different values, such as location, height, and rotation angle. As a result, a total of 364 scenes are created. Then in order to obtain the controlled scenes, we first delimit a polygon area to place the person model, which is named “Region of Interest (ROI)”. The main purpose of this operation is to make each person appear in the desired area. Finally, to enhance diversity of the generated data, weather condition and time are randomly set to simulate the natural variation of illumination in real-world scenarios.

Person Generation. Since persons are the core of re-ID tasks, it is necessary to elaborately describe the person model in the data generation procedure. Firstly, due to the limitation of GTA5, the number of person categories provided by the game is less than 1,000. But we surprisingly find out that the publisher of GTA5 allows players to develop specific person models for non-commercial use to satisfy specific needs. Therefore, in order to create more person identities, we generate additional person models by collecting a large number of add-on person models and using some auxiliary software (*i.e.*, openIV and addonpeds) to implement transformation from game models to synthetic persons, where the person models are collected from Internet and include many movie stars, sports players, historical political figures, *etc.* For each person model, it contains up to 12 variations on the appearance, such as haircut, mask, and clothing. Overall, we adopt the 2369 person models, which have significant differences in skin color, gender, shape, clothes, *etc.*

Furthermore, during the data generation, each person walks along a scheduled route and does a random action in the chosen scene. We set multiple viewpoints in each position and each person has multiple distinctive traits. when human faces may not be easily observed in some viewpoints, it is feasible

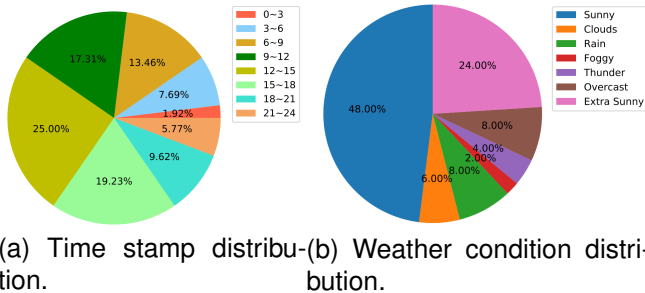


Fig. 2. The pie charts with timestamp and weather condition distribution on our GSPR dataset. In the pie chart 2a, the label "0 ~ 3" represents the time period of [0: 00, 3:00) within 24 hours a day.

to recognize people from other biological characteristics or other viewpoints. Similar to the person re-ID in real-world scenarios, we are able to identify persons by their face, or other characteristics such as gender, age, clothes, and hairstyle from multiple viewpoints.

Data Labeling. The last step is to label the generated samples, where we utilize the hash value of objects provided by GTA5 to determine the identity of each person model. Due to the powerful ability of Mask R-CNN [55] in semantic segmentation, we apply it to automatically detect persons in the generated samples and produce the corresponding bounding boxes. In addition, we also add the information of viewpoints and cameras (locations), which are set as the important parts of the identity label for each sample.

B. Property Analysis for GSPR

Based on the above data generation process, we first construct a large-scale GTA5 synthetic person re-id dataset, namely GSPR, which consists of 739,218 images with 2369 identities. As shown in Table 1, compared with the existing person re-ID datasets, GSPR is a more large-scale synthetic re-ID dataset, both in terms of data volumes and person identities. In addition to these advantages, GSPR is more diverse than existing datasets.

Viewpoint Diversity. GSPR captures 312 viewpoints in the virtual world of GTA5, which are distributed in 26 locations with significant difference, including indoor scenes: bank, museum, pub, parking lot, *etc.*, and outdoor scenes: walking street, plaza, beach and so on. There are 12 viewpoints for each position. Specifically, a person moves freely along a scheduled route, and the camera capture images sequentially from 12 angles at the each position, where all cameras have a high resolution of 1920×1080 . Therefore, the entire GSPR dataset collects 2369 (identities) \times 26 (cameras) \times 12 (angles) = 739,218 images.

Environment Diversity. In order to generate the data that are close to the real-world scenarios, the images are captured at a random time in a day and under a random weather condition. In particular, we select common weathers, namely clear, clouds, rain, foggy, thunder, overcast and extra sunny. Two pie charts in Fig. 2 show the proportional distribution on the time stamp and weather conditions of the GSPR dataset, respectively. It can be found that although we tend to produce



Fig. 3. Some examples in GSPR dataset. The first row represents samples in ideal situations. The second row represents samples in extreme situations, including illumination deficiency, occlusion, low image resolution, and similar but different people (i.e., the samples in red boxes).

more images under common conditions (*e.g.*, daytime and fine-weather scenes), some extreme cases are considered in our GSPR dataset, such as illumination deficiency, low resolution, and collision. Fig. 3 also illustrate some examples in various cases.

C. mini-GSPR

Instead of considering various complex visual factors, we also construct a mini-scale synthetic person re-ID dataset under ideal conditions, referred as mini-GSPR. It consists of 27,040 images from 520 different identities. In mini-GSPR, we select 13 different locations (9 outdoor and 4 indoor scenes), and it is worth noting that there are only four overlapping locations between mini-GSPR and GSPR, including bank, parking lot, sidewalk street, and mountain area. In each location of mini-GSPR, the corresponding camera collects re-ID samples at four angles in sequence. Similar to GSPR, the resolution of cameras in mini-GSPR is 1920×1080 , but mini-GSPR possesses the higher re-ID sample resolution, up to 948×522 . Moreover, all samples in mini-GSPR are generated in the daytime scenes and sunny environment. There is no consideration of extreme cases (*e.g.*, illumination deficiency and occlusion). Compared with GSPR and the existing datasets, mini-GSPR is a more small-scale person re-id dataset in the number of images and the number of identities. However, mini-GSPR is still more diverse in the number of cameras than most datasets in terms of viewpoint and scene, except for MSMT17 and the proposed GSPR, and it has higher sample resolution and ideal visual factors that are difficult to provide in real scenarios. Overall, mini-GSPR dataset contains 520 (identities) \times 13 (cameras) \times 4 (angles) = 27,040 images.

IV. PROPOSED METHOD

In this section, we propose a synthesis-based multi-domain collaborative refinement (SMCR) network for unsupervised cross-domain person re-ID. Specifically, we first give some essential symbolic definitions, and then introduce some components in the SMCR network, including a synthetic pretraining module and two complementary hybrid refinement modules (i.e., DTHR and RIHR). Finally, the proposed SMCR network is further refined by integrating the above modules and performing collaborative training between DTHR and RIHR to

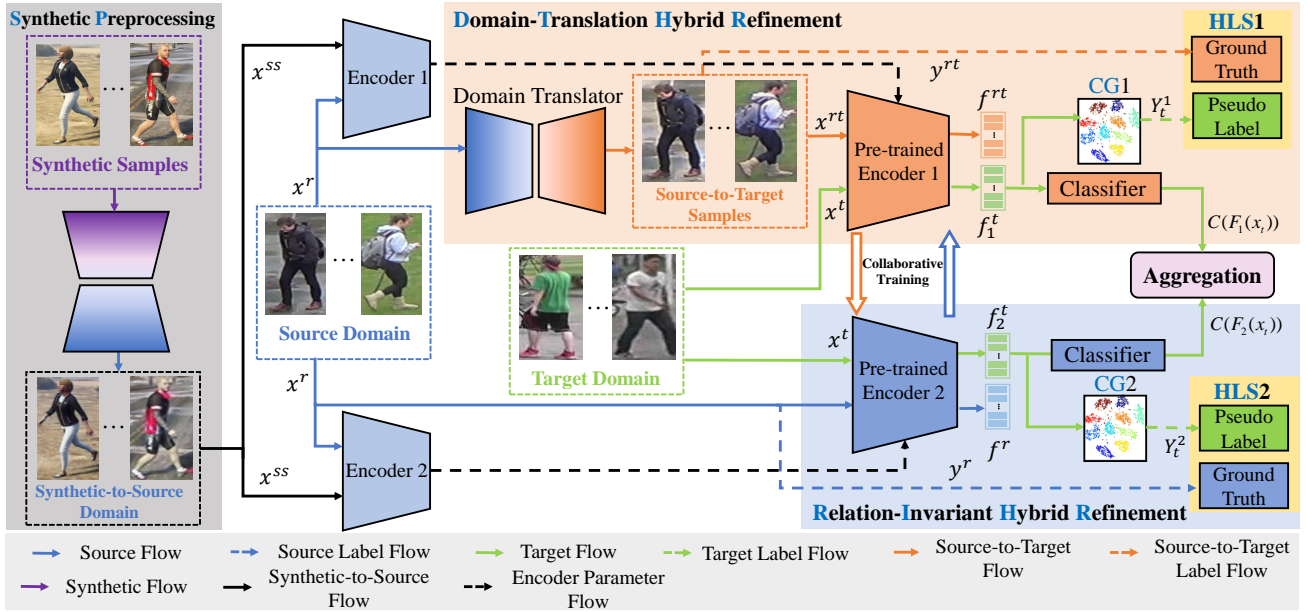


Fig. 4. Overview of our proposed Synthesis-based Multi-domain Collaborative Refinement (SMCR) Network. The overall architecture contains three modules: Synthetic Pretraining, Domain Translation Hybrid Refinement (DTHR), and Relation Invariant Hybrid Refinement (RIHR). **Synthetic Pretraining** module presents a new pretrained scheme to provide better initialization for the domain adaptive model. **DTHR** module integrates the processes of domain translation and pseudo label prediction, and performs joint training for the generated source-to-target samples and target domain data. **RIHR** module maintains original inter-sample relations invariant and implements synchronous learning for source domain and target domain data.

implement sufficient learning for the valuable knowledge from multiple domains. Fig. 4 illustrates the overview framework.

A. Symbolic Definitions

To facilitate understanding, some symbolic definitions are given here. Formally, we first assume access to synthetic data D^S with N_s labeled re-ID samples, where $D^S = \{(x_i^s, y_i^s)\}_{i=1}^{N_s}$. Besides, given the real-world source domain data D^R and target domain data D^T , $D^R = \{(x_i^r, y_i^r)\}_{i=1}^{N_r}$ contains N_r person images with corresponding ground-truth identity labels, and $D^T = \{(x_i^t, \hat{y}_i^t)\}_{i=1}^{N_t}$ involves N_t target images with pseudo labels predicted by the clustering algorithm. Furthermore, we denote source-to-target style-transferred samples as $D^{RT} = \{(x_i^{rt}, y_i^{rt})\}_{i=1}^{N_{rt}}$, in which x_i^{rt} and y_i^{rt} are generated from the source domain data by a domain translator. Similarly, synthetic-to-source style transferred data with D^{SR} can be represented as $D^{SR} = \{(x_i^{sr}, y_i^{sr})\}_{i=1}^{N_{sr}}$.

B. Synthetic Pretraining

Previous methods utilize the pretrained model based on ImageNet or synthetic datasets. However, the pretrained models in the single domain are not the best initialization for domain adaptive tasks. Besides, due to the severe shift between synthetic and real-world data, the model pre-trained on synthetic samples produces dramatic performance deterioration when generalized to real-world datasets.

To this end, a novel pretrained scheme is proposed to remedy the aforementioned problems. On the one hand, to reduce domain discrepancy between synthetic and real data, we translate the generated synthetic data to synthetic-to-source samples by resorting to the generative adversarial network,

where the translated samples enjoy ground-truth identity labels derived from the synthetic data and have a similar style with the source domain. On the other hand, different from the previous methods that solely performed pretraining in a single domain, the designed model is pre-trained both on synthetic-to-source and source domain data, and we regard the pretraining process as performance generalization from synthetic-to-source samples to source domain. In this process, the parameters can be sufficiently trained to meet the needs of domain adaptive tasks in person re-ID, which is much better than traditional pretrained strategies. Finally, the pretrained model is utilized to domain adaptive learning between source domain and target domain.

C. Domain Translation Hybrid Refinement

Conventional UDA methods for person re-ID commonly aim to reduce the negative impacts of domain gap from two different perspectives, performing domain translation to generate source-to-target samples or predicting pseudo labels to refine finetuning in the target domain. However, as mentioned earlier, these methods have some limitations to different extent. To this end, we designed a domain translation hybrid refinement (DTHR) module to consider domain adaptation both in two aspects, which first integrates the processes of domain translation and pseudo label prediction, and then performs joint training with the source-to-target and target domain data during feature encoding. To be specific, as shown in Fig. 4, there are three sub-modules in DTHR, domain translator \mathcal{T} , feature encoder \mathcal{E}_1 , and pseudo-label generator \mathcal{G}_1 . They are parameterized as θ_t , θ_{e1} and θ_{g1} , respectively.

Domain Translator. The domain translator achieves feature translation from the annotated source domain to unlabeled target domain, and generates source-to-target samples with the same ground-truth labels as the source domain and a similar style to the target domain. The translator focuses on maintaining identity-related information invariant during translation, and it is based on the generator from a generative adversarial network. Given a real-world source data pair (x^r, y^r) as input, the corresponding source-to-target sample pair (x^{rt}, y^{rt}) is generated by the domain translator \mathcal{T} , which can be formally expressed as:

$$\begin{cases} x_i^{rt} = \mathcal{T}(x_i^r; \theta_t), & i \in [1, N_{rt}], \\ y_i^{rt} = y_i^r, & i \in [1, N_{rt}]. \end{cases} \quad (1)$$

Because domain translation is not the focus of this paper, we utilize eSPGAN [13] as our domain translator \mathcal{T} in DTHR. The corresponding loss \mathcal{L}_{dt} can be formulated as:

$$\mathcal{L}_{dt} = \mathcal{L}_{\mathcal{T}adv} + \mathcal{L}_{\mathcal{R}adv} + \mu_1 \mathcal{L}_{cyc} + \mu_2 \mathcal{L}_{ide} + \mu_3 \mathcal{L}_c, \quad (2)$$

where the losses $\mathcal{L}_{\mathcal{T}adv}$ and $\mathcal{L}_{\mathcal{R}adv}$ indicate the standard adversarial losses for D^R and D^T , \mathcal{L}_{cyc} denotes the cycle consistency loss, \mathcal{L}_{ide} is the inside-domain identity constraint to preserve the color composition during translation. \mathcal{L}_c is the cross-entropy loss based on the feature learning, which is performed on source-to-target samples using ID-discriminative Embedding (IDE+). Moreover, μ_1 , μ_2 and μ_3 control the relative importance of the corresponding loss, respectively. We recommend referring the readers to CycleGAN [37] and eSPGAN [13] for more detailed information about loss functions.

Feature Encoder. The feature encoder in DTHR is designed to perform joint training for the source-to-target and target domain data, where the extractor is progressively optimized by hybrid learning to provide more discriminative target representation during finetuning. Formally, given a source-to-target image x_i^{rt} and target domain image x_i^t , the corresponding output features $f_{1,i}^t$ and f_i^{rt} of the encoder are obtained by the following mapping:

$$\begin{cases} f_i^{rt} = \mathcal{E}_1(x_i^{rt}; \theta_{e1}), & i \in [1, N_{rt}], \\ f_{1,i}^t = \mathcal{E}_1(x_i^t; \theta_{e1}), & i \in [1, N_t]. \end{cases} \quad (3)$$

Furthermore, in order to implement joint training for source-to-target and target data, we introduce a joint contrastive loss \mathcal{L}_{joint}^1 . It can be defined as:

$$\begin{aligned} \mathcal{L}_{joint}^1 = & -\frac{1}{N_{rt} + N_t} \left(\sum_{i=1}^{N_{rt}} \log \left(\frac{l^1(x_i^{rt})}{\sum_{j=1}^{M_{rt}} l_j^1(x_i^{rt}) + \sum_{j=1}^{M_t^1} l_j^1(x_i^t)} \right) \right. \\ & \left. \cdot y_i^{rt} + \sum_{i=1}^{N_t} \log \left(\frac{l^1(x_i^t)}{\sum_{j=1}^{M_{rt}} l_j^1(x_i^{rt}) + \sum_{j=1}^{M_t^1} l_j^1(x_i^t)} \right) \cdot y_{1,i}^t \right), \end{aligned} \quad (4)$$

$$\begin{cases} l_j^1(x_i^{rt}) = \exp(\langle f_i^{rt}, y_j^{rt} \rangle / \tau), & j \in [1, M_{rt}], \\ l_j^1(x_i^t) = \exp(\langle f_{1,i}^t, y_j^t \rangle / \tau), & j \in [1, M_t^1], \end{cases} \quad (5)$$

where $\langle \cdot, \cdot \rangle$ represents the similarity measure by the inner product for two input feature vectors. τ denotes a temperature hyper-parameter. M_{rt} and M_t^1 are defined as the number of source-to-target sample classes and target domain pseudo categories in DTHR module. Overall, the encoded feature vector is encouraged to close its assigned classes using the above loss during joint training.

Pseudo-label Generator. To implement discriminative feature learning on target domain and remedy the adverse impact of noise pseudo labels, we first predict the pseudo labels for the target domain data using DBSCAN cluster algorithm as the pseudo-label generator \mathcal{G}_1 in DTHR, and then concatenate the predicted pseudo labels and the source ground-truth identity labels to construct a hybrid-label system HLS1. Finally, we refine the predicted pseudo labels by novel cluster criteria, which aims to preserve more reliable data in clusters by measuring the reliability of each feature point during clustering. Concretely, given a feature vector $f_{1,i}^t$, our cluster criteria can be represented as:

$$\begin{cases} c_1(f_{1,i}^t) = \max(0, \frac{|\gamma(f_{1,i}^t) \cap \gamma_s(f_{1,i}^t)|}{|\gamma(f_{1,i}^t) \cup \gamma_s(f_{1,i}^t)|} + \frac{|\gamma(f_{1,i}^t) \cap \gamma_e(f_{1,i}^t)|}{|\gamma(f_{1,i}^t) \cup \gamma_e(f_{1,i}^t)|} - \eta_1), \\ c_2(f_{1,i}^t) = \max(0, \frac{|\gamma(f_{1,i}^t) \cap \gamma_s(f_{1,i}^t)|}{|\gamma(f_{1,i}^t) \cup \gamma_s(f_{1,i}^t)|} - \frac{|\gamma(f_{1,i}^t) \cap \gamma_e(f_{1,i}^t)|}{|\gamma(f_{1,i}^t) \cup \gamma_e(f_{1,i}^t)|} - \eta_2), \end{cases} \quad (6)$$

where $\gamma(f_{1,i}^t)$ denotes the cluster set containing the feature $f_{1,i}^t$, $\gamma_s(f_{1,i}^t)$ and $\gamma_e(f_{1,i}^t)$ are the clusters including $f_{1,i}^t$ when shrinking and enlarging the distance threshold in the DBSCAN algorithm, respectively. Two dynamic thresholds (*i.e.* η_1 and η_2) and two corresponding clustering criteria (*i.e.* $c_1(f_{1,i}^t)$ and $c_2(f_{1,i}^t)$) are obtained by identifying reliable feature points in the clusters on-the-fly. Overall, we analyze the reliability of feature points from target domain data by comparing their clustering results with the results when shrinking and enlarging the threshold distance, respectively. Finally, the corresponding pseudo-label $\hat{y}_{1,i}^t$ can be obtained by the following mapping:

$$\hat{y}_{1,i}^t = \begin{cases} \mathcal{G}_1(f_{1,i}^t; \theta_{g1}), & c_1(f_{1,i}^t) > 0, c_2(f_{1,i}^t) > 0, \\ -1. & otherwise, \end{cases} \quad (7)$$

when $\hat{y}_{1,i}^t = -1$, the corresponding sample is regarded as discrete instances with individual class labels. Therefore, the number of pseudo labels equals $M_c^t + M_o^t$, where M_c^t and M_o^t represent the number of reliable clusters and discrete instances, respectively.

D. Relation Invariant Hybrid Refinement

Although source-to-target data enjoys the similar style to the target domain and remedy the adverse impact of the domain discrepancy, it has been found in [44] that the generated data loses the original inter-sample relations from the source domain after translation.

To this end, we devise a relation-invariant hybrid refinement (RIHR) architecture, which aims to preserve the original inter-sample relations and perform joint learning for source domain and target domain data. As shown in Fig. 4, there is a feature encoder \mathcal{E}_2 and a pseudo-label generator \mathcal{G}_2 in our RIHR module, which have the same structural details as sub-modules in DTHR, but the parameters of these sub-modules

are not shared between DTHR and RIHR. Furthermore, two sub-modules in RIHR are parameterized with θ_{e2} and θ_{g2} , respectively, and we generate a new hybrid-label system HLS2 by concatenating identity labels from the source domain and the new target pseudo label set. These parameterized sub-modules are iteratively trained to obtain the discriminative features in the target domain, where we simultaneously utilize source domain data with inter-sample relations and pseudo-labeled target domain data. Formally, the output feature of the encoder in RIHR can be formulated as:

$$\begin{cases} f_i^r = \mathcal{E}_2(x_i^r; \theta_{e2}), & i \in [1, N_r] \\ f_{2,i}^t = \mathcal{E}_2(x_i^t; \theta_{e2}), & i \in [1, N_t]. \end{cases} \quad (8)$$

The joint contractive loss \mathcal{L}_{joint}^2 is written as:

$$\begin{cases} l_j^2(x_i^r) = \exp(\langle f_i^r, y_j^r \rangle / \tau), & j \in [1, M^R], \\ l_j^2(x_i^t) = \exp(\langle f_{2,i}^t, y_j^t \rangle / \tau), & j \in [1, M^T]. \end{cases} \quad (9)$$

$$\begin{aligned} \mathcal{L}_{joint}^2 = & -\frac{1}{N_r + N_t} \left(\sum_{i=1}^{N_r} \log \left(\frac{l^2(x_i^r)}{\sum_{j=1}^{M_r} l_j^2(x_i^{rt}) + \sum_{j=1}^{M_t} l_j^2(x_i^t)} \right) \right. \\ & \left. \cdot y_i^r + \sum_{i=1}^{N_t} \log \left(\frac{l^2(x_i^t)}{\sum_{j=1}^{M_t} l_j^2(x_i^{rt}) + \sum_{j=1}^{M_r} l_j^2(x_i^t)} \right) \cdot y_{2,i}^t \right). \end{aligned} \quad (10)$$

E. SMCR Network

In order to implement synthesis-based multiple domains collaborative training and refinement, we construct a novel network by assembling the devised synthetic pretraining, DTHR and RIHR modules, referred as SMCR network. We first utilize the abundant information from synthetic samples, source domain and target domain as the input of the SMCR network for jointly learning valuable knowledge from multiple domains. To be specific, for synthetic samples, a novel pretrained scheme is used in the synthetic pretraining module, which provides better initialization for subsequent modules by combining with source domain data; for source domain data, we aim to reduce the negative impact of domain gaps by generating style-transferred samples in DTHR, and the original inter-sample relations invariant is considered by directly learning the source rich information in RIHR; for target domain data, the valuable complementary knowledge is obtained from two branches (*i.e.* DTHR and RIHR) using predicting pseudo labels based on our cluster criteria.

Furthermore, to further remedy the adverse side of the noisy pseudo-labels and optimize the discrimination of target features, we introduce soft pseudo-labels by performing collaborative refinement between the DTHR module and the RIHR module in a mutual-learning manner. To prevent the two modules from converging so close to each other that their output independence is lost, inspired by MoCo [56] and MMT [50], we construct a momentum update encoder for each module to extract discriminative target features as additional soft pseudo-labels for supervising another module. Formally,

the parameters of momentum update encoders from DTHR module and RIHR module at k -th iteration can be indicated as $A^k(\theta_{e1})$ and $A^k(\theta_{e2})$, respectively. They are able to be obtained by:

$$\begin{cases} A^k(\theta_{e1}) = \lambda A^{k-1}(\theta_{e1}) + (1 - \lambda)\theta_{e1}, \\ A^k(\theta_{e2}) = \lambda A^{k-1}(\theta_{e2}) + (1 - \lambda)\theta_{e2}, \end{cases} \quad (11)$$

where $A^{k-1}(\theta_{e1})$ and $A^{k-1}(\theta_{e2})$ are the parameters of momentum update encoders from the two modules at iteration $k - 1$, θ_{e1} and θ_{e2} are updated by back-propagation in each iteration. It is worth noting that we set $A^0(\theta_{e1}) = \theta_{e1}$ and $A^0(\theta_{e2}) = \theta_{e2}$ in first iteration. $\lambda \in [0, 1]$ is a momentum coefficient. Furthermore, we construct a collaborative triple loss between the two modules (*i.e.*, DTHR and RIHR). Given a target domain image x_i^t , the collaborative triple loss L_{col} is able to be formulated as:

$$L_{col} = \alpha L_{col}^1 + (1 - \alpha)L_{col}^2, \quad (12)$$

where L_{col}^1 indicates the collaborative training loss of RIHR's momentum update encoder for the DTHR module and L_{col}^2 is vice versa. The hyper-parameter α controls the contribution from each loss term:

$$\begin{cases} L_{col}^1 = -\frac{1}{N^T} \sum_{i=1}^{N^T} [S(x_i^t, \theta_{e1}) \cdot \log S(x_i^t, A^k(\theta_{e2}))], \\ L_{col}^2 = -\frac{1}{N^R} \sum_{i=1}^{N^R} [S(x_i^t, \theta_{e2}) \cdot \log S(x_i^t, A^k(\theta_{e1}))], \end{cases} \quad (13)$$

$$S(x_i^t, \theta_{e1}) = \frac{\exp(D^+(x_i^t, \theta_{e1}))}{\exp(D^+(x_i^t, \theta_{e1}) + D^-(x_i^t, \theta_{e1}))}, \quad (14)$$

where $S(x_i^t, \theta_{e1})$ represents the softmax triple item generated by DTHR module, and its corresponding soft label is $S(x_i^t, A^k(\theta_{e2}))$ from RIHR module. Furthermore,

$$\begin{cases} D^+(x_i^t, \theta_{e1}) = \|\mathcal{E}_1(x_i^t; \theta_{e1}) - \mathcal{E}_1(x_{i,+}^t; \theta_{e1})\|, \\ D^-(x_i^t, \theta_{e1}) = \|\mathcal{E}_1(x_i^t; \theta_{e1}) - \mathcal{E}_1(x_{i,-}^t; \theta_{e1})\|, \end{cases} \quad (15)$$

where $x_{i,-}^t$ and $x_{i,+}^t$ indicate the hardest positive and negative samples for the input x_i^t in a mini-batch. $D^-(x_i^t, \theta_{e1})$ and $D^+(x_i^t, \theta_{e1})$ are the Euclidean distance between the feature of x_i^t and the features of $x_{i,-}^t$ and $x_{i,+}^t$, respectively.

At the last stage of SMCR, we perform a weighted average for the learned information from two branches by weighted factor α to further refine the discriminative ability of the model, and the averaging results are regarded as the final outputs of the SMCR network. Therefore, given target domain image x_i^t , the corresponding final output y_i of SMCR network is:

$$\begin{aligned} y_i = & \alpha \mathcal{C}_1(f_{1,i}^t) + (1 - \alpha) \mathcal{C}_2(f_{2,i}^t) \\ = & \alpha \mathcal{C}_1(\mathcal{E}_1(x_i^t; \theta_{e1})) + (1 - \alpha) \mathcal{C}_2(\mathcal{E}_2(x_i^t; \theta_{e2})), \end{aligned} \quad (16)$$

where \mathcal{C}_1 and \mathcal{C}_2 are two learnable classifiers from DTHR and RIHR to predict person identity label.

The overall loss function combines the joint training losses (*i.e.*, \mathcal{L}_{joint}^1 and \mathcal{L}_{joint}^2) from the DTHR module and the RIHR module with the collaborative triple loss using hyper-

parameters α and β , which can be defined as:

$$\mathcal{L} = \beta \mathcal{L}_{col} + 2(1 - \beta)(\alpha \mathcal{L}_{joint}^1 + (1 - \alpha) \mathcal{L}_{joint}^2). \quad (17)$$

V. EXPERIMENTS

In this section, we first introduce the experimental datasets and implementation details. Then the experimental results of the proposed SMCR network on four domain adaptive person re-ID tasks are shown, and we compare them with state-of-the-art methods. Finally, the effectiveness of all the components is examined using the ablation study.

A. Datasets and Implementation Details

Datasets. The proposed approach is evaluated on five person re-ID datasets, including the proposed GSPR and mini-GSPR, real-world datasets Market-1501 [3], DukeMTMC-reID [4] and MSMT17 [5]. The Market-1501 [3] dataset consists of 32,668 annotated images of 1,501 identities shot from 6 cameras in total, for which 12,936 images of 751 identities are used for training and 19,732 images of 750 identities are in the testset. DukeMTMC-reID [4] contains 16,522 person images of 702 identities for training, and the remaining images out of another 702 identities for testing, where all images are collected from 8 cameras. Meanwhile, DukeMTMC-reID considers additional 408 identities as distractors. MSMT17 [5] is the most challenging and large-scale real-world dataset consisting of 126,441 bounding boxes of 4,101 identities taken by 15 cameras, for which 32,621 images of 1,041 identities are spitted for training. But it is worth noting that MSMT is collected from 180 hours of high-resolution videos and three labelers annotated it for two months. Such costs are unaffordable in real-world application deployment. Comparatively, GSPR only spent 156 CPU-hours and mini-GSPR took 52 CPU-hours.

Implementation Details. We adopt the IBN-ResNet50 as the backbone of our feature encoders (*i.e.* \mathcal{E}_1 and \mathcal{E}_2), which is proposed by [63] and aims to strengthen generalization capacity of deep neural networks for domain adaptative tasks. The training parameters include 50 epochs, batch size 64, momentum 0.2, and weight decay 0.0005. We initialize the learning rate to be 0.00035 and decrease it by 10 every 20 epochs. For two dynamic thresholds (*i.e.* η_1 and η_2) in cluster criterion, they are set to the sum and difference of the top-90% $\frac{|\gamma(f^t) \cap \gamma_s(f^t)|}{|\gamma(f^t) \cup \gamma_s(f^t)|}$ in the first epoch and the maximum $\frac{|\gamma(f^t) \cap \gamma_e(f^t)|}{|\gamma(f^t) \cup \gamma_e(f^t)|}$ in the cluster of each epoch. The hyperparameters λ and β in our SMCR network are set to 0.5 and 0.01, respectively. Besides, we adopt mean average precision (mAP) and CMC Rank-1, Rank-5, Rank-10 accuracies to evaluate the performance of models. It is worth noting that the predicted pseudo labels for the fine-tuning are updated after each epoch, so the mini-batch of target-domain images have to be re-organized with updated pseudo labels after each epoch. All images are resized to 256×128 when they are ready to feed into the networks. We conduct all experiments on 4 GTX-1080TI GPUs, and there are no post-processing technologies (*e.g.* re-ranking and multi-query fusion) in our experiments.

B. Comparison with State-of-the-arts.

We compare our proposed approach with state-of-the-art UDA methods on four unsupervised cross-domain re-ID tasks in Table II. In order to illustrate the effectiveness of the synthetic pretraining module in the proposed method, we use the constructed synthetic datasets GSPR and mini-GSPR to participate in model pretraining, and the pretrained models are called ‘‘SMCR (GSPR)’’ and ‘‘SMCR (mini-GSPR)’’, respectively. It can be seen in Table II that our SCMR network implements significantly performance improvements when comparing with state-of-the-art methods in terms of mAP and CMC Rank-1, Rank-5, Rank-10 accuracies.

Specifically, we first verify the performance of our SCMR network by comparing it with domain translation-based approaches. SDA [44] used an online relationship consistency regularization term in a compact model to perform domain translation and maintain inter-sample relations invariant, which dominate state-of-the-art performance in domain translation-based methods. However, the proposed SMCR network surpasses SDA by a big margin. SCMR (mini-GSPR) obtains relative improvements of 8.1% (82.4% vs 74.3%), 6.5% (73.2% vs 66.7%), 9.5% (32.7% vs 23.2%) mAP and 3.6% (33.9% vs 30.3%) mAP on Market-1501 \rightarrow DukeMTMC-reID, Market-1501 \rightarrow DukeMTMC-reID, Market-1501 \rightarrow MSMT17 and DukeMTMC-reID \rightarrow MSMT17 domain adaptive tasks, respectively. SMCR (GSPR) gains further performance improvements against SDA by 8.7%, 7.0%, 9.6%, and 4.4% mAP on the four domain adaptive tasks. These results demonstrate the effectiveness of our SMCR network to learn valuable domain adaptive knowledge by enhancing domain translation in DTHR and maintaining inter-sample relations in RIHR.

We then evaluate the performance of the SMCR network and report the comparison results about pseudo-label-based methods. Due to remarkable performance, pseudo-label-based methods have been a hot research topic in the field of UDA for person re-ID. Recently, ABMT [62] gains optimal performance by using an asymmetric structure inside teacher-student networks. Comparing with ABMT, SMCR (mini-GSPR) still implements performance improvements by 2% (82.4% vs 80.4%), 2.4% (73.2% vs 70.8%) and 4.9% (32.7% vs 27.8%), and 0.9% (33.9% vs 33.0%) mAP on four domain adaptation tasks. Furthermore, the performance of SMCR (GSPR) yields new records on the unsupervised cross-domain person re-ID problem. These results show that the proposed method is able to provide more discriminative feature learning capacity using our cluster criteria and collaborative refinement.

C. Ablation Study

1) *UDA from Synthesis to Real:* To further verify the effectiveness of the constructed synthetic datasets for unsupervised domain adaptive person re-ID, we perform the UDA experiments from the labeled synthetic datasets (*i.e.*, GSPR and mini-GSPR) to three unlabeled public real-world datasets: Market1501, DukeMTMC-ReID, and MSMT17. In these UDA experiments, the synthetic pretraining module is removed in the SMCR network, and we use synthetic data as the source domain to implement domain adaptation from

TABLE II

COMPARISON OF OUR SMCR NETWORK WITH STATE-OF-THE-ART METHODS ON UNSUPERVISED DOMAIN ADAPTIVE PERSON RE-ID. WE USE BOLD FONTS TO HIGHLIGHT THE BEST RESULTS.

Methods		DukeMTMC-reID \rightarrow Market-1501				Market-1501 \rightarrow DukeMTMC-reID			
		mAP	Rank-1	Rank-5	Rank-10	mAP	Rank-1	Rank-5	Rank-10
SSG [49]	ICCV'19	58.3	80.0	90.0	92.4	53.4	73.0	80.6	83.2
MMCL [48]	CVPR'20	60.4	84.4	92.8	95.0	51.4	72.4	82.9	85.5
ECN++ [57]	TPAMI'20	63.8	84.1	92.8	95.4	54.4	74.0	83.7	87.4
DG-Net++ [58]	ECCV'20	63.8	78.9	87.8	90.4	61.7	82.1	90.2	92.7
JVTC+ [59]	ECCV'20	67.2	86.8	95.2	97.1	66.5	80.4	89.9	92.2
GPR [60]	ECCV'20	71.5	88.1	94.4	96.2	65.2	79.5	88.3	91.4
SDA [44]	arXiv'20	74.3	89.7	95.9	97.4	66.7	79.9	89.1	92.7
MMT [50]	ICLR'20	76.5	90.9	96.4	97.9	67.3	80.8	90.3	93.0
SPCL [47]	NeurIPS'20	79.2	91.5	96.9	98.0	69.9	83.4	91.0	93.1
GLT [61]	CVPR'21	79.5	92.2	96.5	97.8	69.2	82.0	90.2	92.8
ABMT [62]	WACV'21	80.4	93.0	-	-	70.8	83.3	-	-
SMCR (<i>mini-GSPR</i>)		82.4	92.8	97.1	98.3	73.2	85.3	91.9	94.1
SMCR (<i>GSPR</i>)		83.0	93.5	97.2	98.3	73.7	84.8	93.1	94.7

Methods		Market-1501 \rightarrow MSMT17				DukeMTMC-reID \rightarrow MSMT17			
		mAP	Rank-1	Rank-5	Rank-10	mAP	Rank-1	Rank-5	Rank-10
SSG [49]	ICCV'19	8.5	25.3	36.3	42.1	13.3	32.2	-	51.2
ECN+ [57]	TPAMI'20	15.2	40.4	53.1	58.7	16.0	42.5	55.9	61.5
JVTC+ [59]	ECCV'20	25.1	48.6	65.3	68.2	27.5	52.9	70.5	75.9
SDA [44]	arXiv'20	23.2	49.5	62.2	67.7	30.3	59.6	71.7	76.2
GLT [61]	CVPR'21	26.5	56.6	67.5	72.0	27.7	59.5	70.1	74.2
MMT [50]	ICLR'20	26.6	54.4	67.6	72.9	29.7	58.8	71.0	76.1
SPCL [47]	NeurIPS'20	26.8	53.7	65.0	69.8	31.8	58.9	70.4	75.2
ABMT [62]	WACV'21	27.8	55.5	-	-	33.0	61.8	-	-
SMCR (<i>mini-GSPR</i>)		32.7	57.8	70.6	75.2	33.9	60.4	72.8	77.3
SMCR (<i>GSPR</i>)		32.8	58.3	70.7	75.7	34.7	64.9	74.8	78.3

synthetic samples to real-world datasets. The results are shown in Fig. III.

To be specific, the UDA performance of our SMCR network from synthetic to real-world datasets is largely improved over the current state-of-the-art results (AMBT in WACV'21) between real-world datasets, and it is comparative with the performance of our SMCR network for domain adaptive tasks between real-world datasets. Moreover, our SMCR network establishes a state-of-the-art record of the UDA task from GSPR to MSMT17 dataset. We argue that since GSPR and MSMT17 are the largest-scale person re-ID datasets in the virtual world and the real scenarios, respectively, the re-ID model can be fully trained when using GSPR instead of other small datasets. There is no apparent performance gap

when leveraging mini-GSPR and GSPR as source domains, respectively, which indicates that mini-GSPR is able to help achieve remarkable performance improvements with a small data volume through delicate design. It is worth noting the above results are gained without any manual annotation during domain adaptation, which demonstrates the application potential of our constructed synthetic datasets.

2) *Components Effectiveness*: In order to verify the effectiveness of each component in the proposed SCMR network, we create a baseline model by directly applying the backbone (*IBN-ResNet50*) pretrained in the labeled source domain to conduct fine-tuning on the unlabeled target domain, while comparing the results of the baseline, the different components and SCMR network on DukeMTMC-reID \rightarrow Market-1501

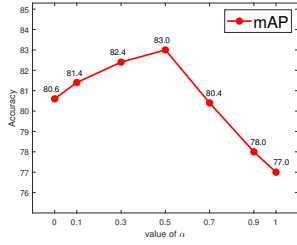
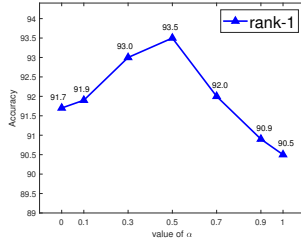
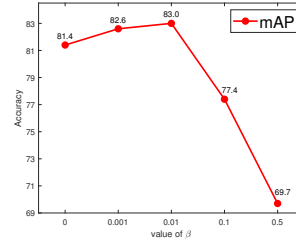
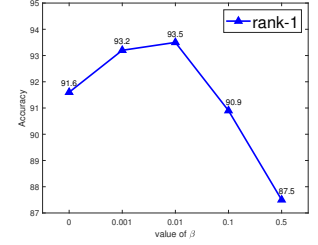
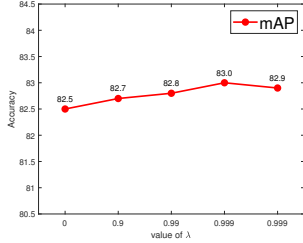
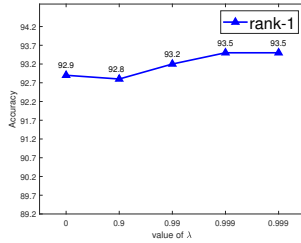
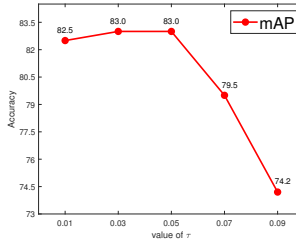
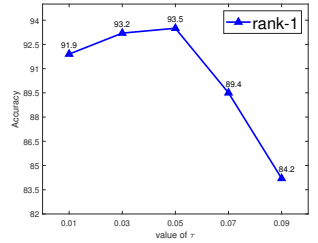
(a) Impact of α for mAP(b) Impact of α for Rank-1 accuracy(c) Impact of β for mAP accuracy(d) Impact of β for Rank-1 accuracy(e) Impact of λ for mAP(f) Impact of λ for Rank-1 accuracy(g) Impact of τ for Rank-1 accuracy(h) Impact of τ for Rank-1 accuracy

Fig. 5. Performance analysis of the proposed SMCR with different values of hyperparameters (*i.e.*, α , β , λ and τ) on Market-1501 \rightarrow DukeMTMC-reID in terms of mAP and Rank-1 accuracies.

TABLE III

PERFORMANCE OF OUR SMCR NETWORK FOR UDA TASKS FROM SYNTHETIC DATASETS TO REAL-WORLD DATASETS.

Source domain	Target domain	mAP	Rank-1	Rank-5	Rank-10
mini GSPR	Market-1501	80.9	91.3	96.4	97.7
	DukeMTMC-ReID	71.2	83.4	91.2	93.2
	MSMT17	34.2	61.2	73.0	77.4
GSPR	Market-1501	81.8	92.2	96.7	97.7
	DukeMTMC-ReID	72.6	84.2	91.0	93.5
	MSMT17	36.1	62.3	73.9	78.0

task. All results are shown in Table IV.

Necessity of Collaborative Refinement. To explore the necessity of collaborative refinement in the proposed SMCR network, we analyze the performance of DTHR module and RIHR module in the mutually independent training manner (*i.e.*, *ind*) and the collaborative training way (*i.e.*, *col*). Significant improvement of 5.1% and 1.3% mAP can be obtained when we collaboratively train the devised DTHR module and RIHR module. Furthermore, it is obvious that the performance difference between DTHR module and RIHR module is significantly reduced when the independent manner is replaced with collaborative training. These results indicate the necessity of the collaborative refinement strategy for module learning and optimization.

Impacts of Different Sub-modules. To further analyze the value of sub-modules of DTHR module and RIHR module,

TABLE IV

ABLATION STUDY OF OUR PROPOSED SMCR NETWORK.

Methods	DukeMTMC-reID \rightarrow Market-1501			
	mAP	Rank-1	Rank-5	Rank-10
Baseline	32.9	61.7	77.1	82.0
DTHR (<i>ind</i>)	77.0	90.5	96.1	97.4
RIHR (<i>ind</i>)	80.6	92.0	97.1	98.2
DTHR (<i>col</i>)	81.3	82.2	92.7	97.2
RIHR (<i>col</i>)	82.2	92.7	97.2	98.0
SMCR (<i>w/o criteria</i>)	47.5	70.2	85.1	89.4
SMCR (<i>ResNet50</i>)	77.8	90.9	96.2	97.6
SMCR (<i>CycleGAN</i>)	80.3	91.4	96.8	98.2
SMCR (<i>w/o syn</i>)	81.8	91.9	97.0	98.0
SMCR (<i>GSPR-pre</i>)	81.0	92.1	96.7	98.1
SMCR (<i>mini-GSPR</i>)	82.4	92.8	97.1	98.3
SMCR (<i>GSPR</i>)	83.0	93.5	97.2	98.3

firstly, we evaluate the effectiveness of cluster criteria, and considerable performance drops (35.5% mAP) are observed when removing our cluster criteria. Then to verify the effectiveness of different backbones for the performance of our SMCR network, we replace IBN-ResNet50 with ResNet50 as the backbone of our feature encoders. There is 4.3% mAP drop for the ResNet50 backbone. Finally, CycleGAN is considered as the domain translator to investigate the impacts of domain translator. Compared with eSPGAN, a relative decrease of

4.9% mAP are shown for the CycleGAN domain translator. Moreover, although the above models have different sub-modules missing, all of them still significantly better than the baseline model. Overall, these results demonstrate the irreplaceability of sub-modules.

Effectiveness of Synthetic Pretraining. To verify testify the signification of our pretrained scheme for the performance of our SMCR network, firstly, we simply removed the synthetic pretraining module in our SCMR, namely SCMR (*w/o syn*). Although SCMR (*w/o syn*) produces a significant performance degradation compared to SCMR (*GSPR*), it is still better than the current state-of-the-art results. Then SCMR (*GSPR-pre*) is constructed by only leveraging the original GSPR samples as pretraining data, where the performance of SCMR (*GSPR-pre*) is even lower than SCMR (*w/o syn*) due to severe shift between synthetic and real-world datasets. Finally, there is only 0.6% mAP performance difference between GSPR (*GSPR*) and GSPR (*mini-GSPR*), which verifies the effectiveness of mini GSPR once again.

3) *Parameter Analysis*: Finally, to evaluate the impact of different hyperparameters, we perform extensive experiments on the task of DukeMTMC-reID \rightarrow Market-1501 by tuning the value of the single parameter and keeping the others fixed. All results can be found in Fig. 5.

Balance coefficient α . In Fig. 5a and 5b, we analyze the effect of the balance coefficient α between DTHR module and RIHR module in Eq. 12, 16 and 17, where the weight for DTHR module is α and the weight for RIHR module is $(1-\alpha)$. Our proposed SCMR network obtains the best results when α is set to 0.5. When β is close to 0 or 1, the performance continues to decrease. These results show that both DTHR and RIHR modules play an indispensable role in feature learning for our SCMR network.

Weighting factor β . Similar to the analysis of α , we testify the proposed framework with different values of the weighting factor β of collaborative losses in Eq. 17. As shown in Fig. 5c and 5d, the values of β varies in 0, 0.001, 0.01, 0.1 and 0.5. Our SCMR network gains the optimal performance with $\beta=0.01$. It can be observed that there is a significant decline when $\beta \geq 0.01$ and disastrous results were obtained with $\beta = 0.5$. Therefore, there is no need to testify the performance of our SCMR network with $\beta=1$. These results indicate that although collaborative training has a certain positive effect on the multi-branch model, it can only be used as an auxiliary strategy.

Momentum Coefficient λ . Inspired by MoCo [56], momentum update encoders are also introduced in our proposed method, and we use momentum coefficient $\lambda = 0.999$ in Eq. 11. Moreover, the performance of our SCMR network is evaluated when tuning $\lambda = 0, 0.9, 0.99$ and 0.9999 , respectively. As demonstrated in Fig. 5e and 5f, we find that our framework gains the best results both on mAP and Rank-1 with $\lambda = 0.999$, and there is a limited impact on performance for momentum update encoders.

Temperature coefficient τ . As shown in Fig. 5c and 5d, we further testify to the performance of our SCMR network by varying the value of temperature coefficient τ in Eq. 5 and 9. Similar to recent methods [64], [57], using temperature



Fig. 6. Query examples on a) Market-1501, b) DukeMTMC-reID and c) MSMT17. For each example, we retrieve rank-10 images from the gallery, where green boxes indicate correct retrievals and the red ones represent wrong cases.

function, our method obtains the optimal results with $\tau = 0.05$, and there is a dramatic decline when $\tau \geq 0.05$.

4) *Qualitative Analysis*: Finally, to qualitatively analyze the performance of the proposed SCMR network, we show some query examples of SCMR network on Market-1501 [3], DukeMTMC-reID [4] and MSMT17 [5]. As shown in Fig. 6, the SCMR network achieves remarkable retrieval performance even for the challenging person samples, where the proposed method can correctly retrieve the person images with significant pose and viewpoint variations, and it is robust to occlusions and background clutter.

VI. CONCLUSION

In this work, we focus on alleviating labeled data severe dependence and poor performance of domain adaptive tasks in the field of person re-identification via synthetic data. To this end, we first develop an automatic data collector/labeler and

construct two synthetic person re-ID datasets with different scales, which do not need any manual labels and free humans from heavy data collections and annotations. In order to further exploit the generated synthetic data, we propose a synthesis-based multi-domain collaborative refinement (SMCR) network to sufficiently absorb the valuable knowledge from multiple domains by performing synthetic pretraining and collaborative refinement. Extensive experiments demonstrate the proposed method achieves consistent performance gains over the state-of-the-art approaches on multiple unsupervised domain adaptation tasks of person re-ID.

In future work, we will focus on self-supervised learning for the re-ID task, which often needs more data and may implement better results. Moreover, it is desirable to generalize domain adaptive learning via synthetic data from image-based to video-based.

REFERENCES

- [1] K. He, X. Zhang, S. Ren, and J. Sun, "Deep residual learning for image recognition," in *Proceedings of the IEEE conference on computer vision and pattern recognition*, 2016, pp. 770–778.
- [2] C. Szegedy, W. Liu, Y. Jia, P. Sermanet, S. Reed, D. Anguelov, D. Erhan, V. Vanhoucke, and A. Rabinovich, "Going deeper with convolutions," in *Proceedings of the IEEE conference on computer vision and pattern recognition*, 2015, pp. 1–9.
- [3] L. Zheng, L. Shen, L. Tian, S. Wang, J. Wang, and Q. Tian, "Scalable person re-identification: A benchmark," in *Proceedings of the IEEE conference on computer vision and pattern recognition*, 2015, pp. 1116–1124.
- [4] E. Ristani, F. Solera, R. Zou, R. Cucchiara, and C. Tomasi, "Performance measures and a data set for multi-target, multi-camera tracking," in *European Conference on Computer Vision*, 2016, pp. 17–35.
- [5] L. Wei, S. Zhang, W. Gao, and Q. Tian, "Person transfer gan to bridge domain gap for person re-identification," in *Proceedings of the IEEE conference on computer vision and pattern recognition*, 2018, pp. 79–88.
- [6] M. Ye, J. Shen, G. Lin, T. Xiang, L. Shao, and S. C. Hoi, "Deep learning for person re-identification: A survey and outlook," *IEEE Transactions on Pattern Analysis and Machine Intelligence*, 2020.
- [7] Y. Lin, Y. Wu, C. Yan, M. Xu, and Y. Yang, "Unsupervised person re-identification via cross-camera similarity exploration," *IEEE Transactions on Image Processing*, vol. 29, pp. 5481–5490, 2020.
- [8] K. Jiang, T. Zhang, Y. Zhang, F. Wu, and Y. Rui, "Self-supervised agent learning for unsupervised cross-domain person re-identification," *IEEE Transactions on Image Processing*, vol. 29, pp. 8549–8560, 2020.
- [9] H. Yao, S. Zhang, R. Hong, Y. Zhang, C. Xu, and Q. Tian, "Deep representation learning with part loss for person re-identification," *IEEE Transactions on Image Processing*, vol. 28, no. 6, pp. 2860–2871, 2019.
- [10] X. Sun and L. Zheng, "Dissecting person re-identification from the viewpoint of viewpoint," in *Proceedings of the IEEE Conference on Computer Vision and Pattern Recognition*, 2019, pp. 608–617.
- [11] I. B. Barbosa, M. Cristani, B. Caputo, A. Rognhaugen, and T. Theoharis, "Looking beyond appearances: Synthetic training data for deep cnns in re-identification," *Computer Vision and Image Understanding*, vol. 167, pp. 50–62, 2018.
- [12] S. Xiang, Y. Fu, G. You, and T. Liu, "Attribute analysis with synthetic dataset for person re-identification," *arXiv preprint arXiv:2006.07139*, 2020.
- [13] W. Deng, L. Zheng, Q. Ye, Y. Yang, and J. Jiao, "Similarity-preserving image-image domain adaptation for person re-identification," *arXiv preprint arXiv:1811.10551*, 2018.
- [14] Y. Chen, X. Zhu, and S. Gong, "Instance-guided context rendering for cross-domain person re-identification," in *Proceedings of the IEEE conference on computer vision and pattern recognition*, 2019, pp. 232–242.
- [15] H. Yu, W. Zheng, A. Wu, X. Guo, S. Gong, and J. Lai, "Unsupervised person re-identification by soft multilabel learning," in *Proceedings of the IEEE conference on computer vision and pattern recognition*, 2019, pp. 2148–2157.
- [16] X. Zhang, J. Cao, C. Shen, and M. You, "Self-training with progressive augmentation for unsupervised cross-domain person re-identification," in *Proceedings of the IEEE International Conference on Computer Vision*, 2019, pp. 8222–8231.
- [17] H. Huang, X. Chen, and K. Huang, "Proxy task learning for cross-domain person re-identification," in *IEEE International Conference on Multimedia and Expo*, 2020, pp. 1–6.
- [18] Y. Zhai, S. Lu, Q. Ye, X. Shan, J. Chen, R. Ji, and Y. Tian, "Ad-cluster: Augmented discriminative clustering for domain adaptive person re-identification," in *Proceedings of the IEEE conference on computer vision and pattern recognition*, 2020, pp. 9021–9030.
- [19] J. McCormac, A. Handa, S. Leutenegger, and A. J. Davison, "Scenenet rgb-d: Can 5m synthetic images beat generic imagenet pre-training on indoor segmentation?" in *Proceedings of the IEEE International Conference on Computer Vision*, 2017, pp. 2678–2687.
- [20] S. Sankaranarayanan, Y. Balaji, A. Jain, S. Nam Lim, and R. Chellappa, "Learning from synthetic data: Addressing domain shift for semantic segmentation," in *Proceedings of the IEEE Conference on Computer Vision and Pattern Recognition*, 2018, pp. 3752–3761.
- [21] Y. Yuan, H. Ning, and X. Lu, "Bio-inspired representation learning for visual attention prediction," *IEEE transactions on cybernetics*, 2019.
- [22] Y. Yuan, D. Wang, and Q. Wang, "Memory-augmented temporal dynamic learning for action recognition," in *Proceedings of the AAAI Conference on Artificial Intelligence*, vol. 33, no. 01, 2019, pp. 9167–9175.
- [23] Q. Wang, J. Gao, W. Lin, and Y. Yuan, "Learning from synthetic data for crowd counting in the wild," in *Proceedings of the IEEE conference on computer vision and pattern recognition*, 2019, pp. 8198–8207.
- [24] Q. Wang, J. Gao, Y. Yuan, and W. Lin, "Pixel-wise crowd understanding via synthetic data," *International Journal of Computer Vision*, vol. 129, no. 1, pp. 225–245, 2021.
- [25] S. Bak, P. Carr, and J.-F. Lalonde, "Domain adaptation through synthesis for unsupervised person re-identification," in *Proceedings of the European Conference on Computer Vision (ECCV)*, 2018, pp. 189–205.
- [26] S. Xiang, Y. Fu, G. You, and T. Liu, "Unsupervised domain adaptation through synthesis for person re-identification," in *2020 IEEE International Conference on Multimedia and Expo (ICME)*, 2020, pp. 1–6.
- [27] B. Sun, J. Feng, and K. Saenko, "Return of frustratingly easy domain adaptation," *arXiv preprint arXiv:1511.05547*, 2015.
- [28] M.-Y. Liu and O. Tuzel, "Coupled generative adversarial networks," in *Advances in Neural Information Processing Systems*, 2016, pp. 469–477.
- [29] H. Ajakan, P. Germain, H. Larochelle, F. Laviolette, and M. Marchand, "Domain-adversarial neural networks," *arXiv preprint arXiv:1412.4446*, 2014.
- [30] Y. Ganin, E. Ustinova, H. Ajakan, P. Germain, H. Larochelle, F. Laviolette, M. Marchand, and V. Lempitsky, "Domain-adversarial training of neural networks," *The Journal of Machine Learning Research*, vol. 17, no. 1, pp. 2096–2030, 2016.
- [31] M. Long, Y. Cao, J. Wang, and M. Jordan, "Learning transferable features with deep adaptation networks," in *International conference on machine learning*, 2015, pp. 97–105.
- [32] E. Tzeng, J. Hoffman, N. Zhang, K. Saenko, and T. Darrell, "Deep domain confusion: Maximizing for domain invariance," *arXiv preprint arXiv:1412.3474*, 2014.
- [33] K. Bousmalis, N. Silberman, D. Dohan, D. Erhan, and D. Krishnan, "Unsupervised pixel-level domain adaptation with generative adversarial networks," in *Proceedings of the IEEE conference on computer vision and pattern recognition*, 2017, pp. 3722–3731.
- [34] J. Hoffman, E. Tzeng, T. Park, J. Zhu, P. Isola, K. Saenko, A. Efros, and T. Darrell, "Cycada: Cycle-consistent adversarial domain adaptation," in *International conference on machine learning*, 2018, pp. 1989–1998.
- [35] T. Kim, M. Cha, H. Kim, J. K. Lee, and J. Kim, "Learning to discover cross-domain relations with generative adversarial networks," *arXiv preprint arXiv:1703.05192*, 2017.
- [36] Z. Yi, H. Zhang, P. Tan, and M. Gong, "Dualgan: Unsupervised dual learning for image-to-image translation," in *Proceedings of the IEEE international conference on computer vision*, 2017, pp. 2849–2857.
- [37] J.-Y. Zhu, T. Park, P. Isola, and A. A. Efros, "Unpaired image-to-image translation using cycle-consistent adversarial networks," in *Proceedings of the IEEE International Conference on Computer Vision*, 2017, pp. 2223–2232.
- [38] M. Chen, K. Q. Weinberger, and J. Blitzer, "Co-training for domain adaptation," in *Advances in Neural Information Processing Systems*, 2011, pp. 2456–2464.
- [39] O. Sener, H. O. Song, A. Saxena, and S. Savarese, "Learning transferable representations for unsupervised domain adaptation," *Advances*

- in *Neural Information Processing Systems*, vol. 29, pp. 2110–2118, 2016.
- [40] W. Zhang, W. Ouyang, W. Li, and D. Xu, “Collaborative and adversarial network for unsupervised domain adaptation,” in *Proceedings of the IEEE Conference on Computer Vision and Pattern Recognition*, 2018, pp. 3801–3809.
- [41] S. Lin, H. Li, C.-T. Li, and A. C. Kot, “Multi-task mid-level feature alignment network for unsupervised cross-dataset person re-identification,” *arXiv preprint arXiv:1807.01440*, 2018.
- [42] J. Wang, X. Zhu, S. Gong, and W. Li, “Transferable joint attribute-identity deep learning for unsupervised person re-identification,” in *Proceedings of the IEEE Conference on Computer Vision and Pattern Recognition*, 2018, pp. 2275–2284.
- [43] W. Deng, L. Zheng, Q. Ye, G. Kang, Y. Yang, and J. Jiao, “Image-image domain adaptation with preserved self-similarity and domain-dissimilarity for person re-identification,” in *Proceedings of the IEEE conference on computer vision and pattern recognition*, 2018, pp. 994–1003.
- [44] Y. Ge, F. Zhu, R. Zhao, and H. Li, “Structured domain adaptation for unsupervised person re-identification,” *arXiv preprint arXiv:2003.06650*, 2020.
- [45] J. Liu, Z.-J. Zha, D. Chen, R. Hong, and M. Wang, “Adaptive transfer network for cross-domain person re-identification,” in *Proceedings of the IEEE Conference on Computer Vision and Pattern Recognition*, 2019, pp. 7202–7211.
- [46] Y.-J. Li, C.-S. Lin, Y.-B. Lin, and Y.-C. F. Wang, “Cross-dataset person re-identification via unsupervised pose disentanglement and adaptation,” in *Proceedings of the IEEE International Conference on Computer Vision*, 2019, pp. 7919–7929.
- [47] Y. Ge, D. Chen, F. Zhu, R. Zhao, and H. Li, “Self-paced contrastive learning with hybrid memory for domain adaptive object re-id,” *Advances in Neural Information Processing Systems*, 2020.
- [48] D. Wang and S. Zhang, “Unsupervised person re-identification via multi-label classification,” in *Proceedings of the IEEE conference on computer vision and pattern recognition*, 2020, pp. 10981–10990.
- [49] Y. Fu, Y. Wei, G. Wang, Y. Zhou, H. Shi, and S. Thomas, “Self-similarity grouping: A simple unsupervised cross domain adaptation approach for person re-identification,” in *Proceedings of the IEEE International Conference on Computer Vision*, 2019, pp. 6112–6121.
- [50] Y. Ge, D. Chen, and H. Li, “Mutual mean-teaching: Pseudo label refinery for unsupervised domain adaptation on person re-identification,” pp. 1–14, 2020.
- [51] H. Fan, L. Zheng, C. Yan, and Y. Yang, “Unsupervised person re-identification: Clustering and fine-tuning,” *ACM Transactions on Multimedia Computing, Communications, and Applications*, vol. 14, no. 4, pp. 1–18, 2018.
- [52] A. Wu, W.-S. Zheng, and J.-H. Lai, “Unsupervised person re-identification by camera-aware similarity consistency learning,” in *Proceedings of the IEEE International Conference on Computer Vision*, 2019, pp. 6922–6931.
- [53] Z. Zhong, L. Zheng, Z. Luo, S. Li, and Y. Yang, “Camera style adaptation for person re-identification,” in *Proceedings of the IEEE Conference on Computer Vision and Pattern Recognition*, 2018, pp. 5157–5166.
- [54] X. Zhu, Z. Luo, P. Fu, and X. Ji, “Voc-reid: Vehicle re-identification based on vehicle-orientation-camera,” in *Proceedings of the IEEE/CVF Conference on Computer Vision and Pattern Recognition Workshops*, 2020, pp. 602–603.
- [55] K. He, G. Gkioxari, P. Dollár, and R. Girshick, “Mask r-cnn,” in *Proceedings of the IEEE international conference on computer vision*, 2017, pp. 2961–2969.
- [56] K. He, H. Fan, Y. Wu, S. Xie, and R. Girshick, “Momentum contrast for unsupervised visual representation learning,” in *Proceedings of the IEEE/CVF Conference on Computer Vision and Pattern Recognition*, 2020, pp. 9729–9738.
- [57] Z. Zhong, L. Zheng, Z. Luo, S. Li, and Y. Yang, “Learning to adapt invariance in memory for person re-identification,” *IEEE Transactions on Pattern Analysis and Machine Intelligence*, 2020.
- [58] Y. Zou, X. Yang, Z. Yu, B. Kumar, and J. Kautz, “Joint disentangling and adaptation for cross-domain person re-identification,” in *European Conference on Computer Vision*, 2020, pp. 87–104.
- [59] J. Li and S. Zhang, “Joint visual and temporal consistency for unsupervised domain adaptive person re-identification,” pp. 1–14, 2020.
- [60] C. Luo, C. Song, and Z. Zhang, “Generalizing person re-identification by camera-aware invariance learning and cross-domain mixup,” pp. 1–8, 2020.
- [61] K. Zheng, W. Liu, L. He, T. Mei, J. Luo, and Z.-J. Zha, “Group-aware label transfer for domain adaptive person re-identification,” *Proceedings of the IEEE conference on computer vision and pattern recognition*, 2021.
- [62] H. Chen, B. Lagadec, and F. Bremond, “Enhancing diversity in teacher-student networks via asymmetric branches for unsupervised person re-identification,” in *Proceedings of the IEEE/CVF Winter Conference on Applications of Computer Vision*, 2021, pp. 1–10.
- [63] X. Pan, P. Luo, J. Shi, and X. Tang, “Two at once: Enhancing learning and generalization capacities via ibn-net,” in *European Conference on Computer Vision*, 2018, pp. 464–479.
- [64] Z. Zhong, L. Zheng, Z. Luo, S. Li, and Y. Yang, “Invariance matters: Exemplar memory for domain adaptive person re-identification,” in *Proceedings of the IEEE conference on computer vision and pattern recognition*, 2019, pp. 598–607.



Qi Wang (M'15-SM'15) received the B.E. degree in automation and the Ph.D. degree in pattern recognition and intelligent systems from the University of Science and Technology of China, Hefei, China, in 2005 and 2010, respectively. He is currently a Professor with the School of Artificial Intelligence, Optics and Electronics (iOPEN), Northwestern Polytechnical University, Xi'an 710072, P.R. China. His research interests include computer vision and pattern recognition.



Sikai Bai received the B.E. degree in software engineering from China University Of Geosciences, Wuhan, China, in 2019. He is currently working toward the M.S. degree in the School of Computer Science and School of Artificial Intelligence, Optics and Electronics (iOPEN), Northwestern Polytechnical University, Xi'an 710072, P.R. China. His research interests include computer vision and pattern recognition.



Junyu Gao received the B.E. degree and the Ph.D. degree in computer science and technology from the Northwestern Polytechnical University, Xi'an 710072, Shaanxi, P. R. China, in 2015 and 2020, respectively. He is currently an Assistant Professor with the School of Artificial Intelligence, Optics and Electronics (iOPEN), Northwestern Polytechnical University, Xi'an 710072, P.R. China. His research interests include computer vision and pattern recognition.



Yuan Yuan (M'05-SM'09) is currently a Full Professor with the School of Artificial Intelligence, Optics and Electronics (iOPEN), Northwestern Polytechnical University, Xi'an 710072, Shaanxi, P. R. China. She has authored or co-authored over 150 papers, including about 100 in reputable journals, such as the IEEE TRANSACTIONS AND PATTERN RECOGNITION, as well as the conference papers in CVPR, BMVC, ICIP, and ICASSP. Her current research interests include visual information processing and image/video content analysis.